Marine Pollution Bulletin 86 (2014) 443–457

Contents lists available at ScienceDirect

Marine Pollution Bulletin

journal homepage: www.elsevier.com/locate/marpolbul

A three-step model to assess shoreline and offshore susceptibility to oil spills: The South Aegean (Crete) as an analogue for confined marine basins

Tiago M. Alves [a,*], Eleni Kokinou [b], George Zodiatis [c]

[a] 3D Seismic Lab, School of Earth and Ocean Sciences, Cardiff University, Main Building-Park Place, Cardiff CF10 3AT, United Kingdom
[b] Technological Educational Institute Crete, Department of Environmental & Natural Resources Engineering, 3 Romanou Str. Chalepa, Chania, Crete GR 73133, Greece
[c] Oceanography Centre, University of Cyprus, P.O. Box 20537, 1678 Nicosia, Cyprus

ARTICLE INFO

Article history:
Available online 10 August 2014

Keywords:
Oil-spill predictions
GIS
Shoreline susceptibility
Bathymetry
Geology
Oceanography

ABSTRACT

This study combines bathymetric, geomorphological, geological data and oil spill predictions to model the impact of oil spills in two accident scenarios from offshore Crete, Eastern Mediterranean. The aim is to present a new three-step method of use by emergency teams and local authorities in the assessment of shoreline and offshore susceptibility to oil spills. The three-step method comprises: (1) real-time analyses of bathymetric, geomorphological, geological and oceanographic data; (2) oil dispersion simulations under known wind and sea current conditions; and (3) the compilation of final hazard maps based on information from (1) and (2) and on shoreline susceptibility data. The results in this paper show that zones of high to very-high susceptibility around the island of Crete are related to: (a) offshore bathymetric features, including the presence of offshore scarps and seamounts; (b) shoreline geology, and (c) the presence near the shore of sedimentary basins filled with unconsolidated deposits of high permeability. Oil spills, under particular weather and oceanographic conditions, may quickly spread and reach the shoreline 5–96 h after the initial accident. As a corollary of this work, we present the South Aegean region around Crete as a valid case-study for confined marine basins, narrow seaways, or interior seas around island groups.

1. Introduction

Accidental oil spills account for 10–15% of all oil that enters the world's oceans, the major source of anthropogenic marine pollution being land-based discharges (European Environmental Agency, 2013). Yet, oil spills derived from maritime accidents, or from oil and gas platforms, comprise a major environmental and financial threat to local communities, particularly when resulting in the release large volumes of unrefined hydrocarbons, or crude oil, to the sea (Palinkas et al., 1993a; Arata et al., 2000; Gill et al., 2012; Sammarco et al., 2013). A particular issue with large oil spill accidents is that their impact significantly increases in confined marine basins, where spill arrival times to the shoreline are relatively short. This vulnerability of confined basins is further enhanced by significant demographic and environmental pressures, with the livelihood of coastal populations depending on sea resources, tourism and in the maintenance of open maritime routes (Danovaro et al., 1995; Peters et al., 1999; Pavlakis et al., 2001; Kingston, 2002). In these regions, large oil spills also challenge the best-laid contingency plans, as clean-up and recovery operations require a great number of specially trained emergency teams (Doerffer, 1992; De la Huz et al., 2005; Kirby and Law, 2010).

One of the most widely documented examples of the impact of oil spills on relatively confined, environmentally sensitive shorelines is the *MV Exxon Valdez* accident of 1989, South Alaska (Petterson et al., 2003). The effects of the *MV Exxon Valdez* on biodiversity, and on the health of the cleaning personnel, were felt in the Prince William Sound for decades after its sinking (Palinkas et al., 1993b; Piatt and Anderson, 1996; Petterson et al., 2003). Nevertheless, the published literature chiefly refers to open-sea accidents such the *Deepwater Horizon* explosion in the Gulf of Mexico (Camili et al., 2010; Kessler et al., 2011), or the *MV Prestige* and *MV Erika* oil spills in the North Atlantic Ocean (Tronczynski et al., 2004; Franco et al., 2006; Gonzalez et al., 2006). This narrow pool of information poses important constraints to emergency authorities, as open sea

* Corresponding author. Tel.: +44 02920876754.
E-mail addresses: alvest@cardiff.ac.uk (T.M. Alves), ekokinou@chania.teicrete.gr (E. Kokinou), gzodiac@ucy.ac.cy (G. Zodiatis).

http://dx.doi.org/10.1016/j.marpolbul.2014.06.034
0025-326X/© 2014 The Authors. Published by Elsevier Ltd.

accidents require emergency responses distinct from oil spills occurring in topographically confined seas. Oil spills in open seas have the potential to unfold relatively slowly, but spreading through large areas to hinder any spill containment procedures (see Galt et al., 1991; Carson et al., 1992). In contrast, oil spills in confined marine basins will potentially reach the shoreline in just a few hours, as shown by the models in this paper, but potentially dispersing through relatively small areas.

In the topographically confined Mediterranean Sea, to quickly assess shoreline susceptibility to oil spill accidents is paramount to the management of human resources and emergency plans by civil protection authorities. Moreover, the coordination of emergency teams in all countries bordering the Mediterranean Sea requires a swift methodology to predict oil spill spreading, dispersion and advection in sea water. This paper presents a new method to help emergency-team response to oil spills in confined marine basins, using the island of Crete as a case-study (Fig. 1a and b). The method was developed under the umbrella of European Commission's NEREIDs project to assist local authorities operating in Crete and Cyprus, Eastern Mediterranean Sea. The method results from the urgent need to coordinate local authorities and civil protection groups in this region when of maritime and offshore platforms accidents. Such a need is particularly pressing at a time when hydrocarbon exploration and production are being equated in deep-water regions of the Eastern Mediterranean (Cohen et al., 1990; Roberts and Peace, 2007).

This paper uses a three-step approach to assess shoreline and offshore susceptibility for two (2) accident scenarios chosen by their proximity to oil and gas depots (Kaloi Limenes) and heavily populated areas (Ierapetra), both in Southern Crete (Fig. 1b). We combine oceanographic, bathymetric and geological data to: (a) assist emergency response plans and (b) to predict the behaviour and fate of oil spilled in the marine environment.

The paper starts with a summary of the past behaviour of oil slicks in the Mediterranean Sea. After listing the new datasets and methodologies utilised, we review the geological setting of Crete prior to presenting the results of our shoreline susceptibility analysis and oil spill modelling. Later in this work, we discuss guidelines for oil-spill mitigation in coastal areas, and the importance of the South Aegean as a case-study for confined maritime basins. We compare and discuss the two accident scenarios modelled with hypothetical scenarios for Northern Crete (Heraklion). Part of this discussion on Northern Crete is based on previous risk analyses undertaken by Kassomenos (2004). As discussed later, the proposed accident scenarios result in distinct geographic distributions and time lengths of spilled oil, parameters that influence any subsequent containment and mitigation work. We then propose that potential impacts differ for two distinct oil spills sources; oil spills during drilling operations, and oil spills caused by maritime accidents.

2. Past behaviour of oil spills in the Mediterranean Sea

2.1. Eastern Mediterranean

The semi-arid climate of the Eastern Mediterranean Sea, in which sun irradiation is high and surface sea temperatures reach 30 °C during the summer months (Coppini et al., 2011), can result in the consumption of up to 93% of spilt oil through emulsification and oxidation processes (Burns and Saliot, 1986). In general, rapid in-situ oxidation is expected in warm waters, imposing an important seasonal control on oil movement and advection in the Eastern Mediterranean (see van Vleet and Reinhardt, 1983 for similar data from semi-tropical estuaries). As a result of rapid oxidation during the summer months, there is little evidence of large-scale accumulations of hydrocarbons in shoreline sediments across the Mediterranean Sea. However, locally there are important accumulations of hydrocarbons where burial rates are high or petroleum inputs are large (Burns and Saliot, 1986). In the Cretan Sea, for instance, *in situ* hydrographic observations demonstrated that important amounts of floating tar enter the Cretan Sea through the Khythira Strait, Western Crete (Kornilios et al., 1998) (Fig. 1a).

The July 2006 Lebanon oil spill allowed the acquisition of important data on the holding capacity of sandy and rocky shorelines in the Eastern Mediterranean (Adler and Inbar, 2007; Coppini et al., 2011). For the Lebanon oil spill, the MEDSLIK model predicted almost 80% of the original oil spilled at sea to have landed after six days along the Lebanese and South Syrian coasts (Coppini et al., 2011). In turn, 20% of the original oil was estimated to have been evaporated within the first days after the spill, whereas less than 1% of the oil remained in the sea. Surface currents were recorded as moving to the east and north in July–August 2006, with velocities

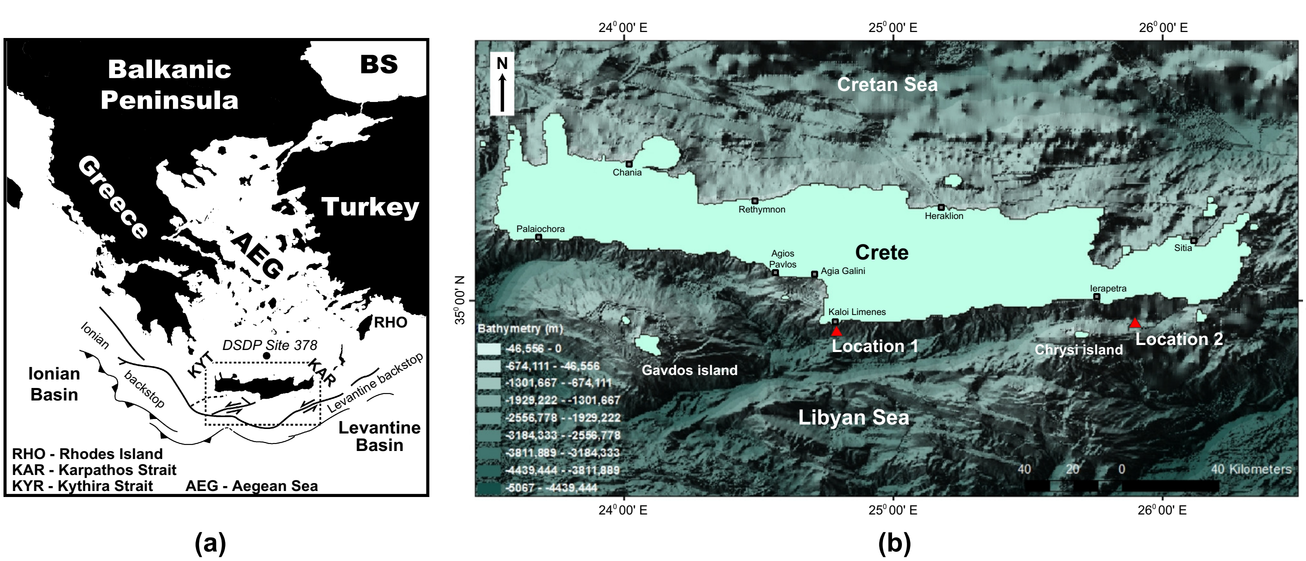

Fig. 1. (a) Location of the study area in the South Aegean Sea. The area considered in this paper is highlighted by the box surrounding the island of Crete. (b) Bathymetric map of the Libyan and Cretan Seas surrounding the island. Note the relative position of Locations 1 and 2 in Southern Crete. Main towns and cities referred to in this paper are highlighted in the figure.

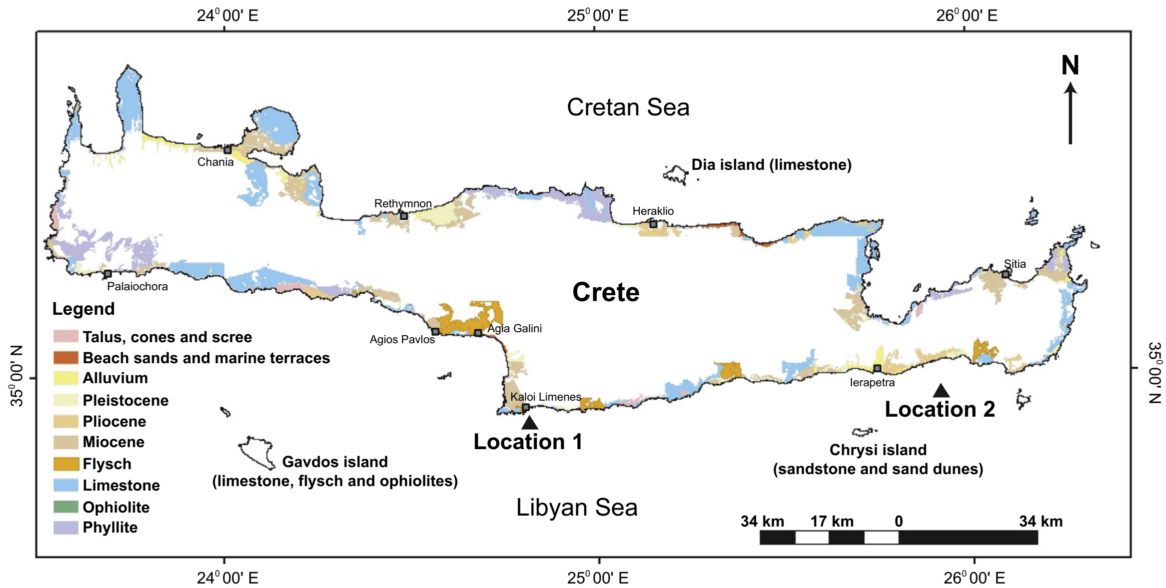

Fig. 2. Shoreline geological map of Crete based on 1:50000 IGME geological maps and Alves et al. (2007). Note the presence of a vast stretch of Tertiary strata and sandy shoreline deposits in both North and Southern Crete, whereas the shorelines of both western and eastern Crete are chiefly composed of hard metamorphic rocks.

ranging from 20 to 30 cm/s in water temperatures as high as 30 °C (Coppini et al., 2011). The high-frequency SKIRON wind forecast system showed winds varying from north-westerly to south-westerly, a pattern that remained steady for most of the summer of 2006, with wind strength varying between 2 and 7 m/s (Lardner et al., 2006).

For these meteorological and oceanographic conditions, oil spill impacts on shoreline regions were observed to be heaviest from Jieh up to south of Beirut, i.e., closer to the spill source. Significant impacts between Beirut and Chekka and northward along the Syrian coast were also reported, and subsequently confirmed several weeks after the oil spill event (Coppini et al., 2011).

2.2. Local cleaning processes

Adler and Inbar (2007) found that sandy shorelines show moderate to low susceptibility to oil spills in areas exposed to significant wave and wind action, i.e., with important natural cleaning processes. Regions with the lower shoreline susceptibility in Israel comprise relatively straight and smooth profiles without deep and complex bays and headlands, preferably low, flat and sandy in nature (Adler and Inbar, 2007). Shoreline susceptibility increases in Israel, and throughout the Mediterranean Sea, with the presence of important ecosystems, specific habitats, coastal resources and shoreline types that must be preserved in case of oil spills.

A contrasting setting is that associated with oil refineries. In Syria and Lebanon, oil refineries were found to be a controlling factor to As and Cr values in seafloor sediment regardless of local wave and meteorological conditions (Othman et al., 2000). Arsenium and Chromium were found to be above natural levels offshore Syria, whereas elements such as Al, Ca, Fe, K, Mg, Mn, Na, Ba and Br and some trace metals (Pb, Zn and Cu) were naturally cleaned and kept under defined limits in the same region. This poses the interesting problem of secondary pollutants in oil spills and, particularly, in industrial (chemical) spills that occur during drilling operations. In this latter case, the North Sea is one of the best documented regions in the literature, and where drilling muds contaminated with hydrocarbons and heavy metal elements are known to be an important polluter (Davies et al., 1984; Grant and Briggs, 2002). Here, hydrocarbon concentration levels were found to be as much as 1000 times normal background levels close to drilling platforms (i.e., at distances < 250 m), but show a rapid decline with distance (Davies et al., 1984). Background levels were found to be reached some 2000–3000 m from the platform, with the shape and extent of polluted zones being largely determined by current regimes and scale of the drilling operations (Davies et al., 1984; Elliot, 1986).

3. Geological and physiographic setting of Crete

3.1. Pre-Miocene core units

The pre-Miocene core of Crete is composed of hard metamorphic rocks, later accreted and eroded to expose several units, the Gavrovo, Plattenkalk, and the phyllite-quartzite unit (Alves et al., 2007; Kokinou et al., 2012). Dominant lithologies include carbonates deposited in neritic (shallow) environments, changing into pelagic (deep-sea) carbonates and flysch, i.e., interbeded sands and shales. Carbonate rocks are vertically stacked and accreted to form a series of tectonic nappes. These nappes are separated by east–west striking structures both onshore and offshore (Alves et al., 2007; Gallen et al., 2014).

3.2. Sedimentology of mapped units in SE Crete

The older post-orogenic formations on Crete are continental sands and conglomerates of possible Burdigalian (Prina Group, Fassoulas, 2001) to Serravalian age (N14 biozone, Postma and Drinia, 1993). In Southeast Crete, limestone-rich breccia-conglomerates are observed above early Tortonian marls and sands with abundant marine fauna (Tefeli Group; van Hinsbergen and Meulenkamp, 2006). The breccia-conglomerates are followed by calcareous sediments, yellow-grey to white marls, evaporites and bioclastic limestones of the Vrysses Group (Fortuin, 1978). These strata are, in turn, overlain by Pliocene/Quaternary sandstones and conglomerates of the Hellenikon and Finikia/Gallini Groups, which in some areas have been uplifted and rotated by active faults.

Shelval sands and muds, uplifted beach rocks and coarse-grained alluvial fans with large scale boulders, are commonly observed on the Cretan shoreline (Fassoulas, 2001; Peterek and Schwarze, 2004; Pope et al., 2008; Alves and Lourenço, 2010).

The modern seafloor offshore Crete is composed of conglomerates and coarse-grained sands intercalated with unconsolidated muds and debris flows within offshore tectonic troughs (Alves et al., 2007; Strozyk et al., 2009).

3.3. Average oceanographic and meteorological conditions

Dominant currents offshore South Crete are west-flowing along the shoreline, and locally influenced by sub-regional gyres and eddies (Malanotte-Rizzoli and Bergamasco, 1991; Theocharis et al., 1993). In contrast, Northern Crete reveals a predominant current direction from northwest to southeast. Periodically, the flow reverses its direction (Zodiatis 1991, 1992, 1993a, 1993b; Triantafyllou et al., 2003). In the Kythira and Karpathos Straits, currents also alternate between northerly and southerly directions (Zodiatis, 1991, 1992, 1993a, 1993b; Theocharis et al., 1999).

Current direction on the Cretan shoreline depends closely on the relative position of water gyres and eddies to the South and North of the island, and on sea-bottom topography (Theocharis et al., 1993, 1999). Quick oil spill dispersion should be expected with strong prevailing winds and strong swells. An important observation is that moderate northerly winds are recorded in Northern Crete during the summer, exposing the shoreline to any major oil spills occurring in the Cretan Sea (Fig. 1b). These same winds are able, in South Crete, to potentially disperse any oil spill away from the island into the Libyan Sea (Fig. 1b).

4. Datasets utilised

The method presented in this work uses the following datasets as the basic information necessary for emergency planning, oil spill prevention and oil spill mitigation.

4.1. Bathymetric data

Bathymetric data from EMODNET were used in this work (Berthou et al., 2008) (Fig. 1b). The EMODNET Hydrography data repository stores Digital Terrain Models (DTM) from selected maritime basins in Europe. DTMs used in this study comprise a grid size of 0.25 min. Each grid cell comprises the following data: (a) *x*, *y* coordinates, (b) minimum water depth in metres, (c) average water depth in metres, (d) maximum water depth in metres, (e) standard deviation of water depth in metres, (f) number of values used for interpolation over the grid cell, (g) number of elementary surfaces used to compute the average grid cell depth, (h) average water depth smoothed by means of a sp line function in metres, and (i) an indicator of the offsets between the average and smoothed water depth as a percentage of water depth.

4.2. Onshore Digital Terrain Models (DTMs)

Onshore topography is amongst the principal parameters used in this study to evaluate shoreline susceptibility. Onshore Digital Terrain Models (DTMs) comprise a 3D digital model of the Earth's surface (McCullagh, 1998; El-Sheimy et al., 2005). For this work, an onshore digital elevation model was created for Crete through the detailed digitization of topographic map contours (1:5000 scale maps) from the Hellenic Military Geographical Service (HAGS) (Fig. 3a). The cell size of the digital elevation model was 20 m.

4.3. Shoreline geological and sensitivity maps

Geological data concerning the near-shore structure and the hydrographic network of Crete were included in the database used in this work. Data sources comprise digital geological maps on the 1:50,000 scale (IGME) and local geological maps completed in the period 2005–2013 (Alves and Lourenço, 2010; Kokinou et al., 2012, 2013). Particular care was taken in the identification of local structures, bed dips, rock and soil quality in the regions where shoreline susceptibility was recognised to be high when of the geological mapping of the shoreline.

Shoreline susceptibility maps were compiled based on field geological data, later complemented by morphological data acquired from Google Maps©. Our susceptibility maps are based on the application of Adler and Inbar (2007) classification, used in Israel to characterise shorelines according to their susceptibility to oil spills and natural cleaning up capacity (Table 1). The Environmental Susceptibility Index (ESI) proposed by Adler and Inbar (2007) considers a range of values between 1 and 9, with level 1 (ESI 1) representing areas of low susceptibility, impermeable to oil spilt during accidents (Table 1). Conversely, ESI 9 shorelines are highly vulnerable, often coinciding with natural reserves and special protected areas (Table 1). As ESI 9 shorelines coincide with such areas of natural importance, data from the updated NATURA 2000 database (http://cdr.eionet.europa.eu/gr/eu/n2000/envujeg6w) were also included in our susceptibility analysis.

4.4. Oceanographic and meteorological data

For the oil spill predictions in the sea area around Crete, sea currents and sea surface temperatures have been acquired from the ALERMO (Aegean Levantine Regional Model) (Korres and Lascaratos, 2003; Sofianos et al., 2006). The ALERMO is downscaling from MyOcean (www.myocean.eu) regional MFS (Mediterranean Forecasting System) (Pinardi et al., 2007; Tonani et al., 2008; Oddo et al., 2010) and covers the Eastern Mediterranean with forecast data every 6 h, with a horizontal resolution of 3 km. Both the MyOcean regional MFS and the downscaled ALERMO model use satellite-derived sea surface altimetry and available in-situ data. Wind data were obtained from SKIRON (Kallos and SKIRON group, 1998a, 1998b, 1998c, 1998d, 1998e, 1998f) as high frequency weather forecasts (every hour with a 5-km horizontal resolution), while wave data were obtained from CYCOFOS every 3 h, with a 10-km horizontal resolution (Galanis et al., 2012; Zodiatis et al., 2014a, 2014b).

5. Methodology

The three-step method proposed in this paper can be summarised as follows:

(1) Bathymetric, geomorphological, geological and oceanographic data for the area of interest are initially acquired and analysed, considering these parameters as key to the dispersion of oil slicks in offshore areas.
(2) In a second step, oil dispersion is simulated using MEDSLIK (Lardner and Zodiatis, 1998; Lardner et al., 2006; Zodiatis et al., 2012b) under certain wind, wave and sea current conditions. The aim is to compute in Step 3 multiple hazard maps for Crete taking into account specific accident scenarios.
(3) Finally, all previous information is integrated in Geographic Information Systems (GIS) to produce the final hazard maps for the study area.

5.1. Step 1 – integration of bathymetric, geomorphological, geological and oceanographic data

In this initial step, the morphological structure of onshore and offshore areas in Crete (Panagiotakis and Kokinou, in press) was analysed using bathymetric, elevation data, and their derivatives

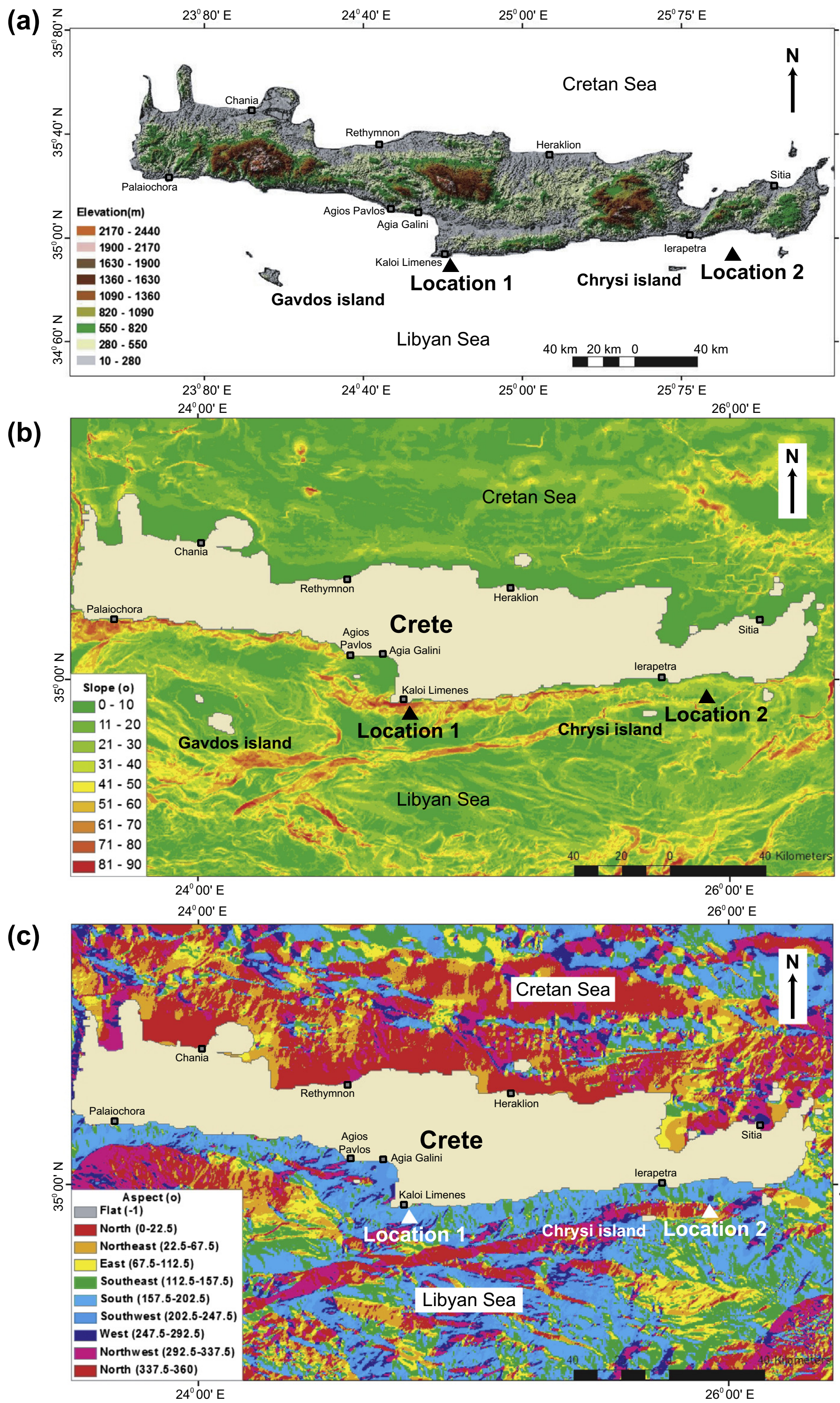

Fig. 3. (a) Onshore elevation map (DTM) for Crete based on data from geological and Hellenic Army charts (see text for details), (b) slope map of the Cretan and Libyan Seas, offshore Crete, as computed from EMODNET bathymetric data, and (c) aspect map computed from EMODNET data following the methodology described in this paper.

(slope and aspect). Our aim was to select the areas of the possible oil spill accidents near to: (a) major sea-bottom features, (b) urban areas with important infrastructures and tourism sites, and (c) coastal regions showing high sensitivity to oil pollution due to their morphology and structure. Slope and aspect features are calculated for each point p of a bathymetric/topographic surface Z using the plane tangent vector $u(p)$:

$$u(p) = \left[\frac{\partial Z(p)}{\partial x}, \frac{\partial Z(p)}{\partial y}\right]^T \tag{1}$$

Slope $S(p)$ is defined as the maximum rate of change in bathymetry or altitude. Thus, the rates of surface change in the horizontal $\frac{\partial Z(p)}{\partial x}$ and vertical $\frac{\partial Z(p)}{\partial y}$ directions from the point p can be used to determine the slope angle $S(p)$:

Table 1
Shoreline Environmental Susceptibility Index (ESI) from Adler and Inbar (2007), representing the susceptibility of particular types of coasts to offshore oil spills.

Environmental Sensitivity Index (ESI)	Shoreline type	Main features and characteristics
ESI 1	Natural, vertical exposed rocky cliffs or headlands; or vertical manmade sea-walls or structures exposed to the open sea	Exposed to the open sea; impermeable to oil; high natural cleanup ability
ESI 2A	Flat abrasion wave cut platforms	Exposed to high wave energy; impermeable to oil (except for very calm and low tide conditions); high natural cleanup ability
ESI 2B	Flat, coarser or slightly sloping exposed platforms created by waves; or low, exposed rocky beaches with larger rocky boulders or structures	Mildly sloping platforms, mostly impermeable to oil; quite high natural cleanup ability
ESI 3	Fine to medium grained sandy beaches, mostly moderately sloping	Low to medium penetration of oil (especially in warm weather); exposed beaches; medium to high natural clean up ability
ESI 4A	Coarse grained sandy beaches, mostly with a steeper slope	Medium penetration and burial of oil; medium natural clean up ability
ESI 4B	Artificial building material dump and/or mixed gravel and small boulders	Low "environmental value" (dump sites of building material); high penetration and burial by oil. Often, oil traps
ESI 5A	Beaches with mixtures of coarse sand, gravel, pebbles and/or shells	Medium to high penetration and burial of oil
ESI 5B	Irregular protrusions of rocks through sand, shells or gravel; or any other irregular, coarse mixture of rocks and unconsolidated sediments	Oil traps in the irregular morphologies; medium to high penetration of oil. Limited natural clean up ability
ESI 6A	Gravel and pebble beaches	Deep penetration and burial of oil (especially in warm weather); exposed to the open sea and high wave energy; limited natural clean up ability
ESI 6B	Man-made, exposed breakwaters extended to the open sea, built of large rocks, rip-rap, or concrete "tetrapodes" or man-made rip rap structures on the beach for coastal protection	High penetration of oil in cracks between boulders, often a trap for large quantities of oil. The side facing the open sea has a high natural clean up ability. If oil penetrates to sheltered areas of the harbour – low natural cleanup ability
ESI 7	Small rivers outlets and "wet" sandy beaches by high ground water	Low penetration of oil; high biological productivity; mostly exposed to the open sea; possible entry of oil into the rivers
ESI 8	Ports and marinas protected by breakwaters or rocky beaches which are protected, or unexposed to the open sea	Areas sheltered from the open sea; irregular surfaces and morphologies. Often traps for large quantities of oil
ESI 9	Beaches with high environmental or biological importance or beaches with other high sensitivity or importance	Nature reserves, specially protected areas, intakes of cooling water for power stations, etc.

$$S(p) = \tan^{-1}\left(|u(p)|_2\right) \qquad (2)$$

where $\tan^{-1}$ is the arctangent function and $|u(p)|_2$is the Euclidean norm of the vector $u(p)$.

Aspect identifies the downslope direction of the maximum rate of change in the value from each point to its neighbours. Therefore, it holds that Aspect can be defined as the slope direction on horizontal plane:

$$A(p) = a\tan 2\left(\frac{\partial Z(p)}{\partial y}, -\frac{\partial Z(p)}{\partial x}\right) \qquad (3)$$

where $a\tan 2$ is the arctangent function with two arguments. The parameter $a\tan 2(y, x)$ is the angle between the positive x-axis of a plane and the point given by the coordinates (x, y) on this same plane. Slope and aspect are measured in this work in degrees with $S(p) \in [0, 90]$ and $A(p) \in [0, 360]$.

The nearshore geology, based on 1:50,000 geological maps (IGME), was complemented with onshore field observations (Alves and Lourenço, 2010; Bathrellos et al., 2012; Kokinou et al., 2013) as well as offshore information (Alves et al., 2007; Kokinou et al., 2012). All information was digitized and included in an ARCGIS database. The location of NATURA 2000 sites were taken from public EU data (http://cdr.eionet.europa.eu/gr/eu/n2000/envujeg6w). Oceanographic inputs for the study area considered a predominant SE–NW current direction, potentially transporting pollutants towards the southwest coast of Crete. Geographic Information Systems (GIS) were used to combine and interpret the datasets and their derivatives. Maps were created using interpolation algorithms, such as Kriging in the initial step, that compute the spatial distribution of specific geological, bathymetric, and oceanographic properties. Kriging is based on statistical models (autocorrelation), variogram modelling, creating the surface, and (optionally) exploring a variance surface.

5.2. Step 2 – MEDSLIK oil spill predictions

The oil-spill model used in this work is the well-established MEDSLIK (Mediterranean oil spill and floating objects predictions) in its latest operational version 5.3.7 (Lardner and Zodiatis, 1998; Lardner et al., 2006; Zodiatis et al., 2012b; Lardner, 2013). The MEDSLIK is a 3D oil-spill model that can predict the transport, fate and weathering of oil spills at any given sea location, or region, upon the availability of oceanographic and weather data. In particular, MEDSLIK has been adapted and used for real incidents, such as the Lebanon oil pollution crisis in summer 2006 (Lardner et al., 2006; World Bank 2007; Coppini et al., 2011), which is considered the largest oil spill accident to ever affect the Eastern Mediterranean. MEDSLIK has been used operationally from 2007 until April 2012 to provide short predictions for any oil spills detected from satellite SAR (Synthetic Aperture Radar) images in the Eastern Mediterranean (Zodiatis et al., 2012b). MEDSLIK is also at the core of the Mediterranean Decision Support System for Marine Safety (www.medess4ms.eu; Zodiatis et al., 2012a), aiming to establish by the end of 2014 a multi model oil-spill prediction service for the entire Mediterranean. This service will use all the available operational oceanographic and atmospheric forecasting data coming from the Copernicus (former GMES-Global monitoring for environment and security) marine service and the national operational oceanographic forecasting systems, as well as data from satellite SAR images and the AIS (Automatic Identifications of Ships). It is of worth to mention that the source code of MEDSLIK has been released and well documented under MEDSLIK-II (De Dominicis et al., 2013a; 2013b), aiming to assist at European level further developments in oil spill prediction modelling.

MEDSLIK incorporates the parameterisation of the oil slick evaporation, emulsification, viscosity changes, dispersion in water column, and adhesion to coast. With MEDSLIK the oil spill is modelled using a Monte Carlo method. The pollutant is divided into a large number of Lagrangian parcels, up to 500,000, of equal size. For this work 100,000 parcels were used, with the size of each parcel being 0.01 m^3. The advective velocity of each oil parcel is a sum of the mean and turbulent fluctuation components of the drift velocity. The advection of the oil slick is caused by the combined action of currents, wind, as well as the Stoke drift. MEDSLIK uses a drift factor approach, which is considered to be the most practical approach for adjusting the advection of the oil slicks coming from low resolution hydrodynamic models. With this method the mean drift velocity of the surface oil is considered to be a weighted sum of the wind velocity and the surface Eulerian velocity field. At each time step, each parcel is given a convective and a diffusive displacement.

The oil spills modelled in MEDSLIK consider a light evaporative component and a heavy non-evaporative component. Emulsification is also simulated, and any viscosity changes in the oil are computed according to the amounts of emulsification and evaporation. Evaporation of the lighter oil fractions follows Mackay et al. (1980b) algorithm, whereas emulsification uses Mackay et al. (1980a) concepts. Beaching on the coast and absorption depending on the type and nature of the shoreline (see Shen et al., 1987 after Torgrimson, 1980). The MEDSLICK model, in addition to its successful use in real oil spill incidents, has received inter-comparison data with other oil spill models using surface drifters (Brostrom et al., 2008; De Dominicis et al., 2010; Zodiatis et al., 2014b).

5.3. Step 3 – compilation of shoreline hazard maps

In a third step, DTM and their derivatives, geological data and the current direction used in oil slick simulations were imported into ArcGIS 10's Iso Cluster Unsupervised Classification package to compile oil spill hazard maps (see Irvin et al., 1997 and Murthy et al., 2003). This is a method of multivariate statistical analysis, searching the relationships among different type of attributes. It is similar to cluster analysis, assigning observations to the same class due to their similar values. It is useful in cases of no pre-existing field data and when the training datasets cannot be accurately specified.

In the analysis in this paper the larger weights have been given to the current direction raster and the derivatives of the DTM, because these parameters control the dispersion of oil spills when an accident occurs near the shore. The output rasters corresponding to the hazard maps of the two selected areas (offshore Ierapetra and in Kaloi Limenes-South Heraklion) are classified in four and five classes respectively and are tied to shoreline sensitivity data (see Section 6). By using hazard maps as such compiled in this work, civil protection agencies can be aware of the exact length of affected shoreline areas, their morphology and degree of access of specific locations to emergency teams.

6. Results

6.1. Bathymetry

It is well known that bathymetry is strongly related to ocean circulation (Marshall, 1995; Whitehead, 1998; Gille et al., 2004), by blocking the water flow and further controlling the direction of the ocean currents, hence the oil spill trajectory. Especially in regions like South Crete, where large fault-bounded scarps are observed offshore, bathymetric features control the amount of the water passing between basins.

Two useful products derived from the analysis of bathymetry data are slope angle and slope aspect plots (Fig. 3b and c). These two types of maps were used in this work to isolate ranges of slope angles for statistical treatment, to identify zones of marked slope instability, and to recognise submarine outcrop exposures. Both datasets (slope angle and slope azimuth) were used to illuminate trends associated with submarine tectonic features (e.g., faults and main ridges). Data from the slope map were grouped in nine classes: (i) 0–10°, (ii) 11–20°, (iii) 21–30°, (iv) 31–40°, (v) 41–50°, (vi) 51–60°, (vii) 61–70°, (viii) 71–80°, and (ix) 81–90° (Fig. 3b). Data from the slope aspect-azimuth maps were grouped in ten classes, varying from flat seafloor areas to features oriented 337–360° (Fig. 3c).

Slope and aspect maps confirmed the presence of important bathymetric features (see also Kokinou et al., 2012). Prevailing slopes in the study areas are greater than 20° steep, while prevailing slope azimuths are 0–40°, 160–200°, 280–320° and 320–359°. It is obvious in South Crete that steep slopes are mainly related to N–S, E–W and WNW–ESE oriented faulting (Kokinou et al., 2012).

6.2. Assessment of shoreline sensitivity

The geomorphology of nearshore areas is an important parameter controlling oil spill advection. In addition, the spatial distribution of contaminants in marine sediments is impacted by natural factors such as parent rock weathering, weather conditions and marine circulation patterns (Rooney and Ledwin, 1989). Marine sediments can, therefore, be a sensitive indicator for both spatial and temporal trend monitoring of contaminants in the marine environment. In this paper, we used geological data from the IGME 1:50,000 digital geological map, new field geological data, high quality aerial imagery from Google Maps© and DTMs from Crete to classify the shoreline of Crete according with the classification in Table 1. Shoreline sensitivity was therefore examined according to Environmental Sensitivity Index (ESI) of Adler and Inbar (2007) for Mediterranean areas (Fig. 4 and Table 1).

Our results show a series of high sensitivity (ESI 9) areas in both north and south Crete. They are related in both regions to the presence of sandy shorelines, with Miocene to Holocene fine sands and muds deposited over older friable sediment of high porosity (Figs. 2, 4 and 5). They also coincide with highly populated areas, regardless of their inclusion, or not, in NATURA 2000 natural reserves (Fig. 5).

6.3. Oil spill spreading and dispersion predictions

Oil spill prediction (Fig. 6) were simulated for South Crete near the natural port of Kaloi Limenes (Location 1), where an oil storage and terminal facility are located, and Ierapetra (Location 2) - comprising a main tourism area. Additionally, these areas were selected based on environmental and demographic criteria (Kassomenos, 2004), as they comprise regions in South Crete where large towns occur, or where NATURA 2000 sites occur close to the shoreline (Fig. 7).

The MEDSLIK oil slick predictions for Locations 1 and 2 present the trajectory of an assumed oil slick with 10,000 tonnes, with a dominant current direction from SE to NW away for the coast to E–W near to the coast (Fig. 6). In the two oil spill models for Locations 1 and 2, the oil slick thickness ranges between 0 and 16.86 mm. In the case of Kaloi Limenes (Location 1, Fig. 6a) the oil slick moved through the Gulf of Tympaki, affecting the coast of Agia Galini as well as part of the eastern coast of Crete. In the case of Ierapetra (Location 2, Fig. 6b), the oil slick affected the low-lying beaches that extend west of Ierapetra (Figs. 4c and 6b). Considering the arrival times for the two cases, the spill arrives to the shore approximately 94 h after the oil spill accident in Kaloi Limenes (Location 1), and 38 h after the accident in Ierapetra (Location 2) (Fig. 6).

6.4. Final hazard maps

The final outcome of the Iso Cluster Unsupervised Classification is a hazard map showing which marine and nearshore areas will be

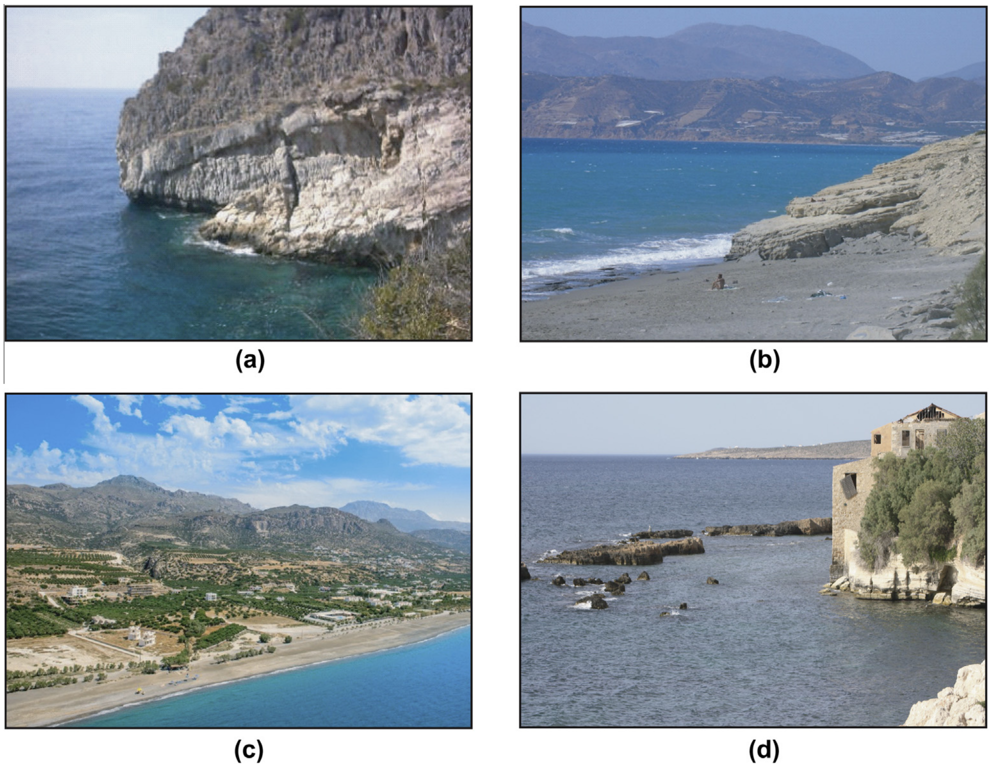

Fig. 4. Examples of shoreline types according to Adler and Inbar (2007) Environmental Susceptibility Index (ESI) classification. (a) ESI 1 shoreline at Agios Pavlos (see Fig. 3 for location) on which vertical rocks exposed to the open sea are observed. These rocks are impermeable to oil and have a high natural cleanup ability. (b) ESI 2A shoreline in the Tympaki Gulf (between Agia Galini and Kaloi Limenes, see Fig. 3 for location). Flat abrasion wave cut platforms, potentially exposed to oil landing from the sea, occur in this region together with coarse-grain sands and pebble beaches. (c) ESI 9 shoreline, Ierapetra beach, gently sloping to the south, and formed over Miocene sands (see Fig. 3 for location). High penetration and burial of oil, but with medium natural clean up ability. (d) ESI 5B shoreline in Chania, showing irregular protrusions of rocks and boulders alternating with unconsolidated sediments (see Fig. 3 for location). This complex shoreline morphology creates oil traps and shows medium to high penetration of oil. ESI 5B shorelines have limited natural clean up ability.

primarily affected in case of an oil spill accident in Locations 1 and 2 (Fig. 8). These maps were compiled taking into account the derivatives of the bathymetry (slope and aspect), geomorphologic factors, and current direction orienting E–W to SE–NW. The division of a probability map into categories was performed for visualization purposes and does not imply a discrete zonation of the study area in safe and unsafe places (Begueria and Lorente, 2003; Lamelas et al., 2008). These values were categorized into five classes for the case of Kaloi Limenes (more sensitive) and four classes for the area of Ierapetra, corresponding to different susceptibility levels (very low, low, moderate, high and very high). In particular, high and very high susceptibility zones are strongly related to bathymetric features, rugged shoreline profiles, and the direction of surface and deeper marine currents.

7. Local effects on end-member scenarios modelled in South Crete

In the early 1980s, over three quarters of a million tonnes of oil were estimated to have been introduced annually into the Mediterranean Sea from land-based and open-sea discharges (Burns and Saliot, 1986). Most of these discharges result from ships navigating in international waters with a minor amount resulting from drilling (Ferraro et al., 2007; European Environmental Agency, 2013). This paper considers two distinct case-studies, one located close to a main depot where maritime accidents may happen (Location 1), and a second case-study (Location 2) where exploratory drilling might be considered in the future (Fig. 8).

Published work in Alves et al. (2007) and Kokinou et al. (2012) demonstrated the existence of a complex depositional setting south of Crete where coarse-grained sediment sourced from dense (hyperpycnal) flows during flash-flood events mostly bypass the short continental shelf into adjacent tectonic troughs. Recognised sedimentary processes during these flash-flood conditions include high-density turbidity flows, and hyperpycnal flows sourced from streams and gorges striking north–south on Crete (Fig. 5). In such a setting, local wind and precipitation conditions have a pronounced effect on proximal near-shoreline conditions.

Comprising a narrow continental shelf, except on the Messara Basin and between Ierapetra and Gaiduronissi, northerly wind conditions during flash-flood events will potentially move any oil spills away from South Crete, at the same time reducing the effect of oil spills on local communities until the moment they reach the continental shelf. In contrast, southerly winds in relatively dry conditions will shorten the time necessary for an oil spill to reach the shoreline. In both situations, the rugged continental slope of South Crete, and intermediate to deep-water current conditions, will potentially form barriers to deeper, sinking oil slicks. The distribution of deep, sunken oil will mainly depend on seasonal currents flowing in tectonic troughs at the time of the oil spill. In the absence of significant upwelling currents along the continental slope of South Crete, the velocity in which the oil slick(s) will sink is an important factor, as sinking slicks will be trapped in tectonic troughs with the steep continental slope of Crete creating a barrier to oil dispersion (Figs. 5 and 8).

A contrasting setting to Southern Crete occurs in the northern half of the island. The continental slope is much broader here, at places culminating in a wide shelf region extended in a SSW–NNE along the island (Fig. 1b). The seafloor offshore Heraklion, for instance, opens to the north forming a gentle continental slope.

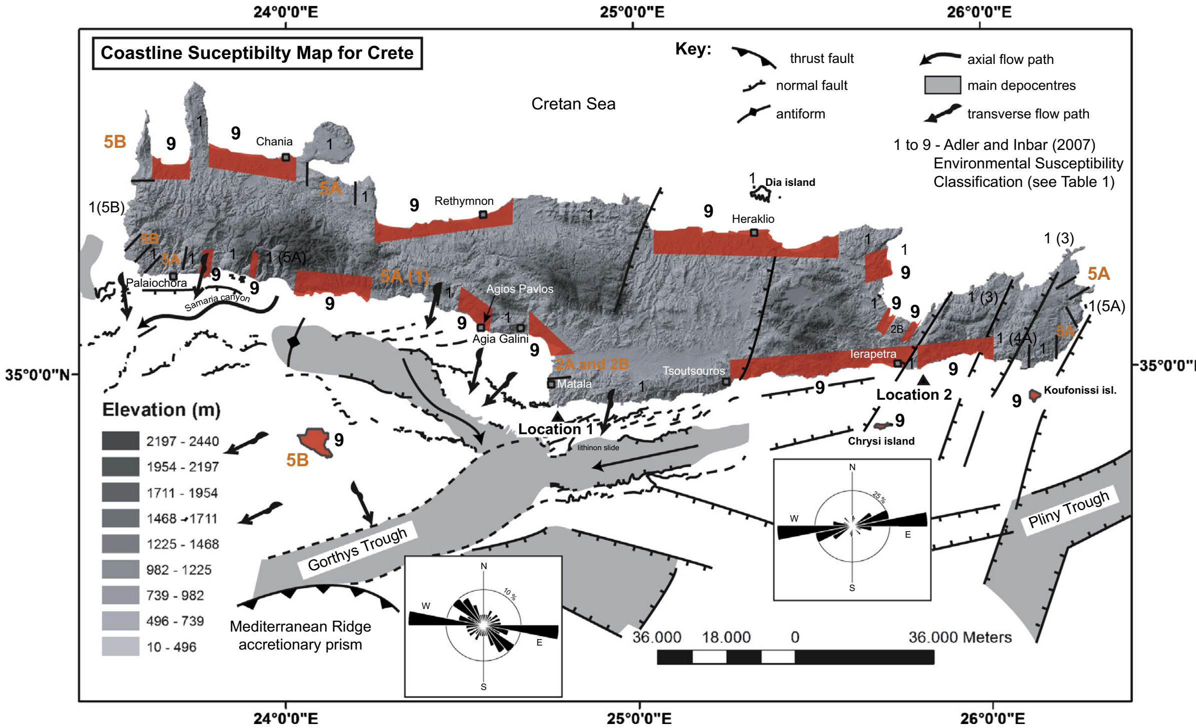

Fig. 5. Shoreline susceptibility map showing (in red) the regions of higher susceptibility on Crete. The map was compiled based on geological maps from SE Crete and shoreline analyses based on field data and Google Earth©. See Table 1 for a description of types ESI 1 to ESI 9 according to Adler and Inbar (2007). (For interpretation of the references to colour in this figure legend, the reader is referred to the web version of this article.)

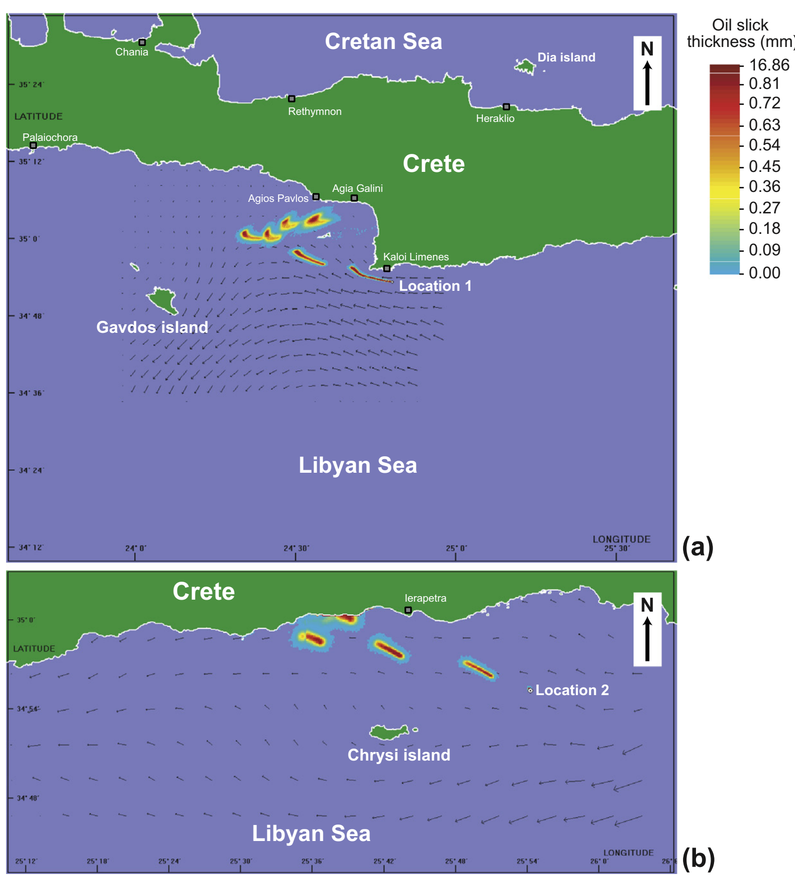

Fig. 6. MEDSLIK oil spill spreading and diffusion models for Locations 1 and 2. Both show a predominant SE–NW spreading direction, with oil spills reaching the shoreline at different times some 5–96 h after the initial accident. Arrows represent surface current vectors for the period analysed.

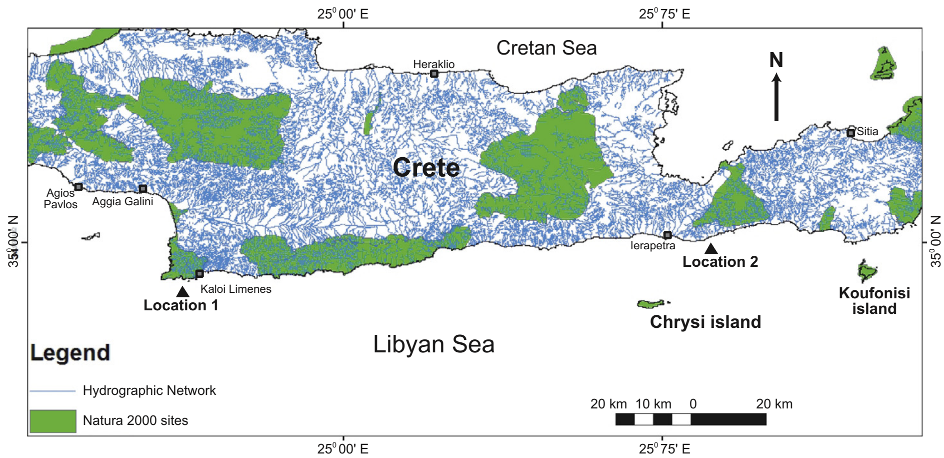

Fig. 7. Location of NATURA 2000 sites on Crete and corresponding hydrographic network.

The average seafloor depth is 35 m some 1.5 km offshore, and is still 50 m deep ~2.0 km from the Northern Crete shoreline (Triantafyllou et al., 2003) (Fig. 1b). Importantly, the shoreline of Northern Crete is sandy to muddy in most of its course, with Holocene sediments resting upon a marly substrate (see Tselepides et al., 2000) of marine origin in the regions were shoreline susceptibility is higher (ESI 9, Fig. 5). In this setting, the vulnerability of the Northern Crete shoreline to any oil spill accident will closely depend on the distance of oil spills to the shore, with close-distance accidents potentially having an immediate impact on shelf and shoreline sediments.

8. Discussion and recommendations

8.1. The South Aegean as a case-study for confined marine basins

The Northern Crete example is that of a gentle continental shelf and slope, such as in parts of North Africa where prevailing winds, surface currents, and a simpler bathymetry may contribute to more moderate rates of oil spill advection. Locations 1 and 2 in South Crete comprise the opposite example, with the existence of complex directions of prevailing winds, submarine currents and topography contributing for less predictable oil spill advection paths. In the straits separating Crete from continental Greece and Turkey, a close dependence of oil spill advection on prevailing current and wind conditions should exist, as these are known to be seasonally variable (Theocharis et al., 1993, 1999).

In Northern Crete, the gentle continental shelf bordering the island contributes to a larger concentration of hydrocarbons close to the shore. Oil dispersion and emulsification might be enhanced if the spill is to form long, linear shapes parallel to the shoreline, sourced from more distant accidents. In contrast, if the spill occurs close to the shoreline it will be important to confine any stranded tanker to a bay or a coastal spit, taking account the dominant wind and current conditions. The aim in this case should be to confine the spill by shoreline topography, taking account shoreline susceptibility and local demography.

Prevalent wind and current conditions are of key importance in confined marine basins. In the worst case scenario large oil spills can rapidly propagate, impacting heavily on islands, spits and bays in Southern Crete. In the case of northerly winds and surface currents, the northern coast of Crete will be in danger, with wind transporting oil slicks towards Crete, while oil spills generated close to the Southern Cretan shore will propagate into the Libyan Sea, where the conditions to dissipate and sink are improved. In the case of prevailing southerly winds, the southern coast of Crete will present the largest risk, while the northern coast will present the lowest risk (e.g., Theocharis et al., 1993, 1999).

Close to the shoreline, decision-makers should avoid any environmentally protected sites, or major cities, using topographic features on the shoreline as a mean to contain the spill. The accessibility of accident areas needs to be taken into account due to the scarcity of major roads. In areas of complex bathymetry, distant oil spills will have the capacity to degrade and sink (Fig. 5). In this case, downwelling and upwelling effects might be significant as controlling factors to the emergence or submergence of oil. Emulsification and dispersion will be higher if wave conditions are rough, as prevailing wave movement is often dependent on currents and winds (Pye, 1992). In gentler slopes as those in Northern Crete, the potential to pollute vast swathes of the seafloor is greater, adding to the susceptibility of the shoreline – already a region with high demographic pressure (Fig. 5). We suggest spill containing procedures to be very swift in case of an oil spill in areas of gentle bathymetry, unless wind and current conditions disperse the slick offshore.

8.2. A guideline for the mitigation of coastal oil spills

The primary questions emergency teams should pose when assessing oil spill scenarios are: (1) who will suffer the impact if an oil spill reaches the shore? (2) will the oil spill, when reaching the shore, impact on areas of significant demographic pressure (e.g., major cities), environmental importance, or both?, and (3) if so, what can be done to mitigate (i.e., reduce) the impact on shoreline ecosystems and populations?

A key factor when addressing Question 1 is oil spill distance to the shoreline (Fig. 9). Previous accidents such as the *MV Prestige* oil spill in 2002 showed that towing operations can be hindered by poor weather conditions, particularly when of remote oil spills that occur far from the shoreline (Balseiro et al., 2003). In the case of the *MV Prestige*, the option taken in November 2002 was to tow the tanker to a distant offshore area where prevailing currents would keep the spill away from the shoreline, allowing for the natural degradation of oil in the Atlantic Ocean (Wirtz and Liu, 2006). The option was taken due to the precarious state of the tanker, which showed substantial hull damage and was in the imminence of sinking. Otherwise, ships should be towed to shoreline areas in which the spill can be contained and oil can be pumped out of containers by mechanical means, if the volume of oil is not overwhelmingly large. National and international environmental laws may apply to specific cases, such as in the USA with the oil pollution Act of 1990 (United States Congress, 1990), but a good

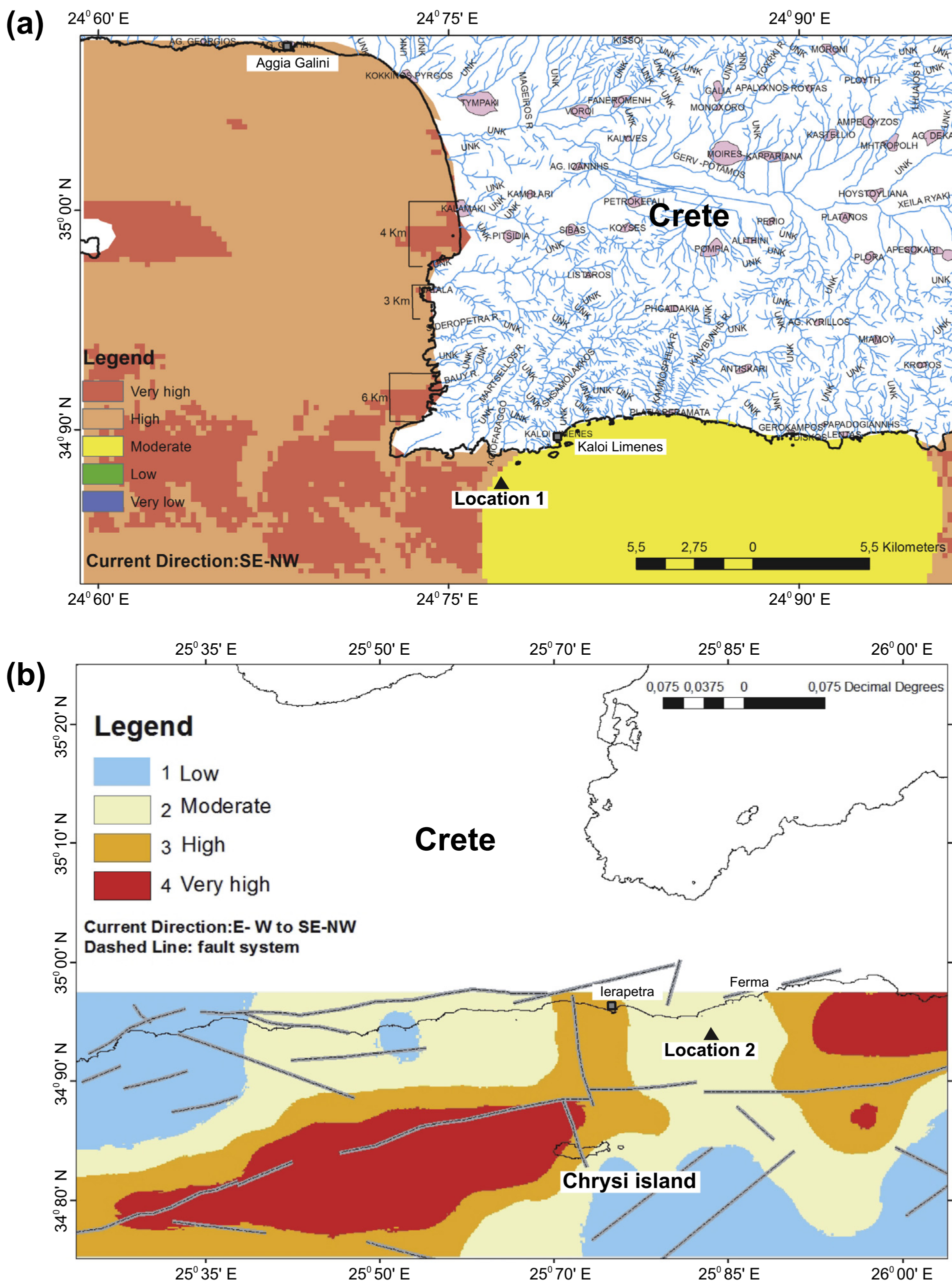

Fig. 8. Oil spill hazard maps indicating the areas where oil spill spreading and diffusion is interpreted to have a larger probability of polluting the shoreline and seafloor bathymetric features in Southern Crete.

example of this latter procedure is the oil spill of 1999 in the Sydney Bay, Australia (MacFarlane and Burchett, 2003). The readily availability of equipment in this harbour allowed the *Laura D'Amato* tanker to remain inside the Shell oil terminal in Gore Cove, with the oil spill being confined to a small area (Sydney Morning Herald, 1999; MacFarlane and Burchett, 2003). Crude oil spilt totalled some 296,000 l during unloading at the terminal of the Shell Co of Australia, but this volume was contained within a small portion of Sydney Bay.

Question 2 depends mainly on the volume and type(s) of oil released to the water and, secondarily, on the volumes reaching the shoreline when of an oil spill (Fig. 9). In this case, two classes of oil spills can be defined: (a) oil spills derived from maritime accidents and (b) oil spills derived from production platforms. The main properties which affect the fate of spilled oil at sea are specific gravity, or its density relative to pure water (often expressed as API* or API gravity); the distillation characteristics of oil slicks (volatility); the viscosity of oil, and the pour point (i.e., the temperature below which the oil slick will not flow). In addition, high wax and asphaltene contents will influence the likelihood of oil mixing with water to form a water-in-oil emulsion (ITOPF, 2013). Oils forming stable oil-in-water emulsions persist longer at the water surface. Typically, oil density is classified in the following groups:

(a) Group I (density < 0.8 g/cm^3), comprising gasoline and kerosene.
(b) Group II (density 0.8–0.85 g/cm^3), gas oil and Abu Dhabi Crude.
(c) Group III (density 0.85–0.95 g/cm^3), Arabian Light Crude, North Sea Crude Oils (e.g., Forties crude).

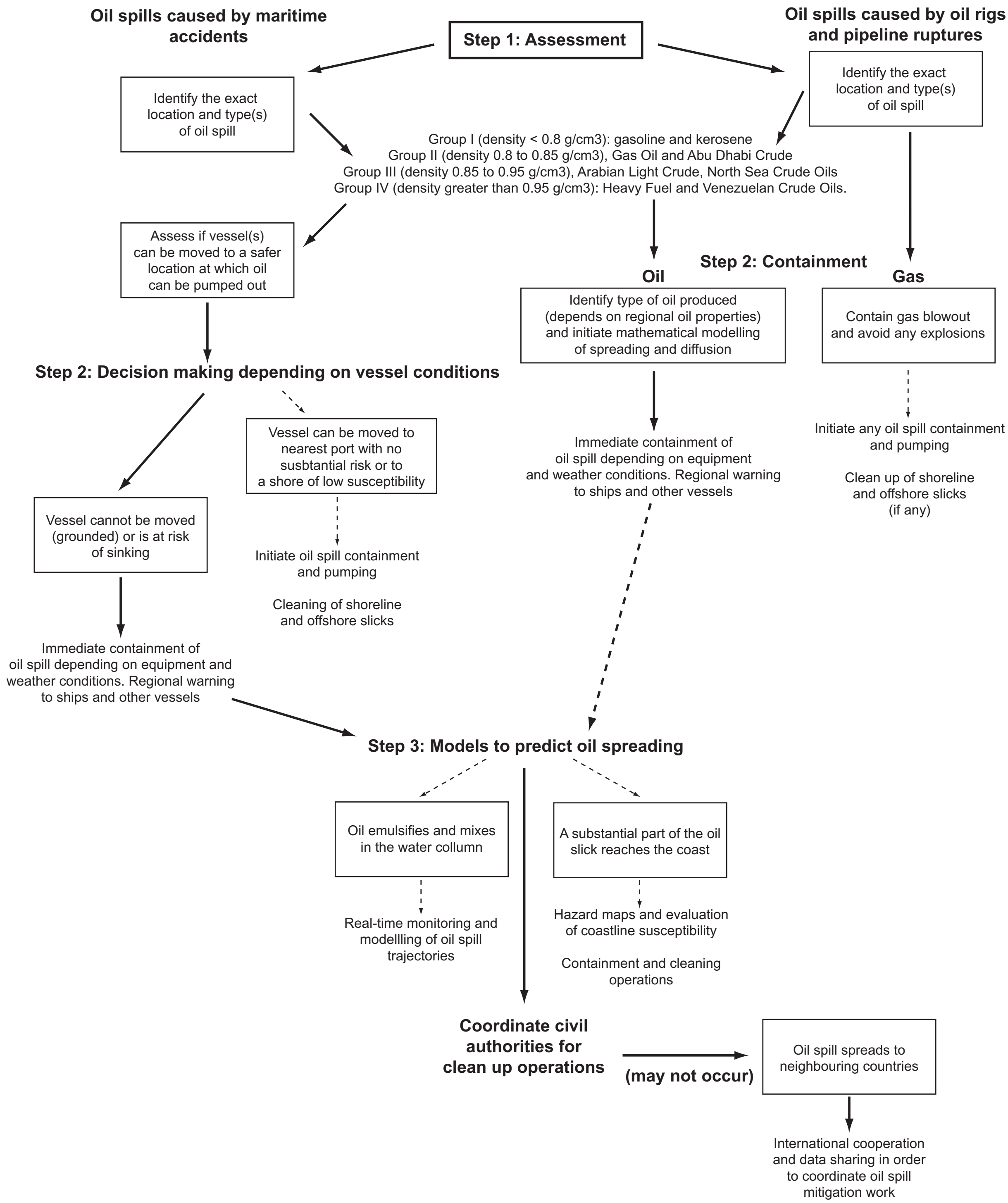

Fig. 9. Workflow suggested in this paper for maritime and platform accidents.

(d) Group IV (density greater than 0.95 g/cm^3), or heavy fuel and Venezuelan Crude Oils.

Group I oils (i.e., non-persistent) tend to dissipate completely through evaporation within a few hours and do not normally form emulsions. Group II and III oils can lose up to 40% by volume through evaporation. Because of their tendency to form viscous emulsions, there is an initial volume increase as well limited natural dispersion, particularly in the case of Group III oils. Group IV oils are very persistent due to their lack of volatile material and high viscosity, which preclude both evaporation and dispersion (ITOPF, 2013).

The volume and type of oil released when of maritime accidents will naturally depend on the type of accident (sinking of oil tanker, with or without hull splitting; grounding of tankers with variable degrees of hull rupture; collision between oil tankers; collision between smaller ships) and on the tonnage of stricken ships. Most of the oil tankers crossing the Mediterranean Sea head to, or from, the Suez Canal – which imposes a tonnage limit of 240,000 deadweight tonnes (DWT) on oil tankers (Suez

Canal Rules of Navigation). However, open sea harbours in the Mediterranean can accommodate ultra large crude carriers with up to 550,000 DWT.

Accidents in production platforms, in contrast, depend closely on local geological conditions and rig equipment (e.g., Deepwater Horizon Investigation Report, 2010) (Fig. 9). In hydrocarbon production stages, accidents are mostly related to pipeline ruptures and explosions on rigs (e.g., Alpha-Piper, Cullen, 1993), with the type of hydrocarbon produced by the platforms being of paramount importance to any spill predictions. Gas blowouts such as the West Vanguard blowout in Norway (October 1985) are capable of releasing large amounts of gas into the water column, but will not result in large oil spills (Sætren, 2007).

Question 3 relates to the response civil protection, governmental institutes, ship and rig operators will provide in the hours after the spill accidents. Based on the experience of two table top exercises for oil spill accidents organised in the context of the NEREIDs project (http://www.nereids.eu/site/en/index.php?file=nereids-project) we suggest the following procedure for specific accidents as a guide to address Question 3:

(a) Ship accidents – evaluate type of accident (grounding, collision, hull rupture), identify type of oil released, and assess distance to shoreline. Consider if towing the ship to harbour or coastal embayment, where shoreline susceptibility is known to be low, are feasible options. Cleaning operations should start immediately upon arrival and should focus on emptying remaining crude from tanks, fuel from ships, and on containing any spills.
(b) Platform accidents – assess type of accident, and if oil is being at all released from platforms or pipelines. Gas platforms accidents result in smaller spills, if any. Accidents on oil production platforms may result in larger accidents if containing equipment malfunctions, or if geological conditions bypass blowout preventers and other machinery. Emphasis should be given on containment, avoiding at the same time any platform explosions.

Finally we suggest cleaning operations to start soon after the spill by using common apparatuses such as booms, skimmers, dredges and pumping vessels (Fig. 9). Bioremediation methods, use of solvents and dispersants, or controlled burning of oil slicks might be options to consider. Due to the long life of hydrocarbons in certain shoreline types, it is imperative that severe measures are taken to address the problem early in the accident(s), at national and international levels, so the impact on marine ecosystems and shoreline populations is mitigated or prevented. Post-spill monitoring of key environmental parameters is therefore crucial to monitor the normal shoreline recovery procedures (Doerffer, 1992; De la Huz et al., 2005; Kirby and Law, 2010).

9. Final concluding remarks

The main conclusion of this work is that the three-step method proposed in this paper allows the definition of regions of higher susceptibility and hazard in case on an oil spill in confined marine basins. The three-step method can be summarised as follows:

(1) Step 1 – bathymetric, geomorphological, geological and oceanographic parameters from the region surrounding the oil spill should be considered as key parameters controlling the dispersion of oil slicks.
(2) Oil dispersion simulations using MEDSLIK are carried out taking into account high-resolution wind, wave and sea current data.
(3) In the third and final step, Geographic Information Systems (GIS) should be used to evaluate the varied factors selected and to compile final shoreline hazard maps.

The compilation of oil spill hazard maps is important to a successful response to oil spill accidents in their early stage. This is because areas of intense urbanization, or environmentally sensitive zones, require an accurate management from civil protection authorities in the very first hours after an oil spill. In the case of an oil spill in deep offshore areas, real-time oceanographic and meteorological data will be paramount to model the path and dispersion rates of oil slicks. As a corollary of this work, the two scenarios modelled show that sea bottom irregularities controlled by the geological structure, as well as coastline morphology and geology, have important impacts on oil spill spreading and dispersion in confined marine basins.

In all models, a final factor to consider is the coupling between the direction of shallow sea currents, wind and wave during rough weather conditions. Changing wind conditions can be an important factor and should be taken into account in oil spill models, as they can allow the movement of oil slicks without affecting the shoreline. Similarly, the effect of the Stoke drift when of rough sea state conditions has to be taken into account, especially close to the shoreline.

Acknowledgements

This work has been co-financed by the EU Humanitarian Aid and Civil Protection under Grant Agreement No. 638494/2012/ECHO/A5/SUB – Project "Embracing Innovation for Preparedness in Civil Protection & Marine Pollution". The authors thank MPB's editor and an anonymous reviewer for their constructive comments.

References

Adler, E., Inbar, M., 2007. Shoreline sensitivity to oil spills, the Mediterranean coast of Israel. Assessment Anal., Ocean Coast. Manage. 50, 24–34.
Alves, T.M., Lourenço, S., 2010. Geomorphologic features related to gravitational collapse: Submarine landsliding to lateral spreading on a Late Miocene-Quaternary slope (SE Crete, eastern Mediterranean). Geomorphology 123, 13–33.
Alves, T.M., Lykousis, V., Sakellariou, D., Alexandri, S., Nomikou, P., 2007. Constraining the origin and evolution of confined turbidite systems: southern Cretan margin, Eastern Mediterranean Sea (34 30–36 N). Geo-Mar. Lett. 27, 41–61.
Arata, C.M., Picou, J.S., Johnson, G.D., McNally, T.S., 2000. Coping with technological disaster: an application of the conservation of resources model to the Exxon Valdez oil spill. J. Trauma. Stress 13, 23–39.
Balseiro, C.F., Carracedo, P., Gómez, P., Leitão, P.C., Montero, P., Naranjo, L., Penabad, E., Perez-Muñizuri, V., 2003. Tracking the prestige oil spill: an operational experience in simulation at MeteoGalicia. Weather 58, 452–458.
Bathrellos, G.D., Gaki-Papanastassiou, K., Skilodimou, H.D., Papanastassiou, D., Chousianitis, K.G., 2012. Potential suitability for urban planning and industry development by using natural hazard maps and geological–geomorphological parameters. Environ. Earth Sci. 66, 537–548.
Begueria, S., Lorente, A., 2003, Landslide hazard mapping by multivariate statistics: comparison of methods and case study in the Spanish Pyrenees. Instituto Pirenaico de Ecologı'a (contract no. EVG1: CT-1999-00007. http://damocles.irpi.pg.cnr.it/ docs/reports/df_modelling.pdf).
Berthou, P. et al., 2008. EMODNET-the European marine observation and data network. Eur. Sci. Found. – Mar. Board, 10.
Brostrom, G., Carrasco, A., Daniel, P., Hackett, B., Lardner, R., Panayidou, X., Paradis, D., Zodiatis, G. 2008. Comparison of different oil drift models and different ocean forcing with observed drifter trajectory in the Mediterranean. In: Coastal to Global Operational Oceanography: Achievements and challenges, 5th EuroGoos Conference proceedings, Sandy Park, Exeter, UK, 20–22 May.
Burns, K.A., Saliot, A., 1986. Petroleum hydrocarbons in the Mediterranean Sea: a mass balance. Mar. Chem. 20, 141–157.
Camili, R., Reddy, C.M., Yorger, D.R., Van Mooy, B.A.S., Jakuba, M.V., Kinsey, J.C., McIntyre, C.P., Sylva, S.P., Maloney, J.V., 2010. Tracking hydrocarbon plume transport and biodegradation at deepwater horizon. Science 330, 201–204.
Carson, R.T., Mitchell, R.C., Hanemann, W.M., Kopp, R.J., Presser, S., Rudd, P.A. 1992. A contingent valuation study of lost passive use values resulting from the Exxon Valdez oil spill. MPRA Paper No. 6984, pp. 452.

Cohen, Z., Kaptsan, V., Flexer, A., 1990. The tectonic mosaic of the southern Levant: implications for hydrocarbon prospects. J. Pet. Geol. 13, 437–462.
Coppini, G., De Dominicis, M., Zodiatis, G., Lardner, R., Pinardi, N., Santoleri, R., Colella, S., Bidnami, F., Hayes, D.R., Soloviev, D., Georgiou, G., Kallos, G., 2011. Hindcast of oil-spill pollution during the Lebanon crisis in the Eastern Mediterranean, July–August 2006. Mar. Pollut. Bull. 62, 140–153.
Cullen, L.W.D. 1993. The public inquiry into the Piper Alpha disaster. Drilling Contractor, 49, OSTI: 6208554.
Danovaro, R., Fabiano, M., Vincx, M., 1995. Meiofauna response to the Agip Abruzzo oil spill in subtidal sediments of the Ligurian Sea. Mar. Pollut. Bull. 30, 133–145.
Davies, J.M., Addy, J.M., Blackman, R.A., Blanchard, J.R., Ferbrachel, J.E., Moore, D.C., Somerville, H.J., Whitehead, A., Wilkinson, T., 1984. Environmental effects of the use of oil-based drilling muds in the North Sea. Mar. Pollut. Bull. 15, 363–370.
De Dominicis, M., Pinardi, N., Fabbroni, N., Coppini, G., Zodiatis, G., Lardner, R. 2010. Oil spill forecasting in the Mediterranean Sea. In: Proceedings of 5th International Conference on EuroGOOS. Coastal to Global Operational Oceanography: Achievements and Challenges, EuroGOOS publication 28, pp. 521–524 (ISBN 978-91-974828-6-8).
De Dominicis, M., Pinardi, N., Zodiatis, G., Archetti, R., 2013a. MEDSLICK-II, a Lagrangian marine surface oil spill model for short-term forecasting – Part 2: numerical simulations and validations. Geosci. Model Dev. 6, 1871–1888.
De Dominicis, M., Pinardi, N., Zodiatis, G., Lardner, R., 2013b. MEDSLICK-II, a Lagrangian marine surface oil spill model for short-term forecasting – Part 1: theory. Geosci. Model Dev. 6, 1851–1869.
De La Huz, L., Lastra, M., Junoy, J., Castellanos, C., Viéitez, J.M., 2005. Biological impacts of oil pollution and cleaning in the intertidal zone of exposed sandy beaches: preliminary study of the "Prestige" oil spill. Estuar. Coast., Shelf Sci. 55, 19–29.
Deep-Water Horizon Investigation Report, 2010, BP, pp. 192.
Doerffer, J.W., 1992. Oil spill response in the marine environment. Elsevier Sci. Technol., 395.
Elliot, A.J., 1986. Shear diffusion and the spread of oil in the surface layers of the North Sea. Deutsche Hydrogr. Zeits. 39, 113–137.
El-Sheimy, N., Valeo, C., Habib, A., 2005. Digital Terrain Modeling: Acquisition, Manipulation and Applications. Artech House Publishers, Boston, p. 270.
European Environmental Agency, 2013, E15 – Accidental oil spills from marine shipping. Indic. Eur. Environ. Agency, E15, pp. 6.
Fassoulas, C., 2001. The tectonic development of a Neogene basin at the leading edge of the active European margin: the Heraklion basin, Crete. Greece J. Geodyn. 31, 49–70.
Ferraro, G., Bernardini, A., David, M., Meyer-Roux, S., Muellenhoff, O., Perkovic, M., Tarchi, D., Topouzelis, K., 2007. Towards an operational use of space imagery for oil pollution monitoring in the Mediterranean basin: a demonstration in the Adriatic Sea. Mar. Pollut. Bull. 54, 403–422.
Fortuin, A.R., 1978. Late Cenozoic history of eastern Crete and implications for the geology and geodynamics of the southern Aegean region. Geol. Mijnbouw.
Franco, M.A., Viñas, L., Soriano, J.A., de Armas, D., González, J.J., Beiras, R., Salas, N., Bayona, J.M., Albalgés, J., 2006. Spatial distribution and ecotoxicity of petroleum hydrocarbons in sediments from the Galicia continental shelf (NW Spain) after the prestige oil spill. Mar. Pollut. Bull. 53, 260–271.
Galanis, G., Hayes, D., Zodiatis, G., Chu, P.C., Kuo, Yu-Heng, Kuo, Yu-Heng, Kallos, G., 2012. Wave height characteristics in the Mediterranean Sea by means of numerical modeling, satellite data, statistical and geometrical techniques. Mar. Geophys. Res. 33, 1–15.
Gallen, S.F., Wegmann, K.W., Bohnenstiehl, D.R., Pazzaglia, F.J., Brandon, M.T., Fassoulas, C., 2014. Active simultaneous uplift and margin-normal extension in a forearc high, Crete, Greece. Earth Plant. Sci. Lett. 398, 11–24.
Galt, J.A., Lehr, W.J., Payton, D.L., 1991. Fate and transport of the Exxon Valdez oil spill. Part 4. Environ. Sci. Technol. 25 (2), 202–209. http://dx.doi.org/10.1021/es00014a001.
Gill, D.A., Picou, J.S., Ritchie, L.A., 2012. The Exxon Valdez and BP oil spills: a comparison of initial social and psychological impacts. Am. Behav. Sci. 56, 3–23.
Gille, S.T., Metzger, E.J., Tokmakian, R., 2004. Topography and ocean circulation. Oceanography 17, 47–54.
Gonzalez, J.J., Viñas, L., Franco, M.A., Fumega, J., Soriano, J.A., Grueiro, G., Muniategui, S., López-Mahía, P., Prada, D., Bayona, J.M., Alzaga, R., Albalgés, J., 2006. Spatial and temporal distribution of dissolved/dispersed aromatic hydrocarbons in seawater in the area affected by the prestige oil spill. Mar. Pollut. Bull. 53, 250–259.
Grant, A., Briggs, A.D., 2002. Toxicity of sediments from around a North Sea oil platform: are metals or hydrocarbons responsible for ecological impacts? Mar. Environ. Res. 53, 95–116.
Irvin, B.J., Ventura, S.J., Slater, B.K., 1997. Fuzzy and isodata classification of landform elements from digital terrain data in Pleasant Valley, Wisconsin. Geoderma 77, 137–154.
ITOPF-International Oil Tankers Pollution Federation, 2013 <http://www.itopf.co.uk/>.
Kallos, G., SKIRON group. 1998. The SKIRON forecasting system: vol. I: preprocessing ISBN 960-8468-15-9.
Kallos, G., SKIRON group. 1998. The SKIRON forecasting system: vol. II: Model description ISBN 960-8468-16-7.
Kallos, G., SKIRON group. 1998. The SKIRON forecasting system: vol. III: Numerical techniques ISBN 960-8468-17-5.
Kallos, G., SKIRON group. 1998. The SKIRON forecasting system: vol. IV: Parallelization ISBN 960-8468-18-3.
Kallos, G., SKIRON group. 1998. The SKIRON forecasting system: vol. V: Post processing ISBN 960-8468-19-1.
Kallos, G., SKIRON group. 1998. The SKIRON forecasting system: vol. VI: Procedures 960–8468-20-5.
Kassomenos, P.A., 2004. Risk analysis for environmental hazards: the case of oil spills, in Crete. Global Nest 6 (1), 39–51.
Kessler, J.D., Valentine, D.L., Redmond, M.C., Du, M., Chan, E.W., Medes, S.D., Quiroz, E.W., Villanueva, C.J., Shusta, S.S., Werra, L.M., Yvon-Lewis, S.A., Weber, T.C., 2011. A persistent oxygen anomaly reveals the fate of spilled methane in the deep gulf of Mexico. Science 331, 312–315.
Kingston, P.F., 2002. Long-term environmental impact of oil spills. Spill Sci. Technol. Bull. 7, 53–61.
Kirby, M.F., Law, R.J., 2010. Accidental spills at sea – risk, impact, mitigation and the need for co-ordinated post-incident monitoring. Mar. Pollut. Bull. 60, 797–803. http://dx.doi.org/10.1016/j.marpolbul.2010.03.015.
Kokinou, E., Alves, T., Kamberis, E., 2012. Structural decoupling on a convergent forearc setting (Southern Crete, Eastern Mediterranean). Geol. Soc. Am. Bull., doi: 10.1130/B30492.1.
Kokinou, E., Skilodimou, H., Bathrellos, G. 2013. Morphotectonic analysis of Hera klion basin (Crete, Greece). In: Bull. Geol. Soc. Greece, Proceedings of the 13th International Congress, pp. 10.
Kornilios, S., Drakopoulos, P.G., Douna, C., 1998. Pelagic tar, dissolved/dispersed petroleum hydrocarbons and plastic distribution in the Cretan Sea, Greece. Mar. Pollut. Bull. 36, 989–993.
Korres, G., Lascaratos, A., 2003. An eddy resolving model of the Aegean and Levantine basins for the Mediterranean Forecasting System Pilot Project (MFSPP): Implementation and climatological runs. Analles Geophysicae 21, 205–220.
Lamelas, M.T., Marinon, O., Hoppe, A., de la Riva, J., 2008. Doline probability map using logistic regression and GIS technology in the central Ebro Basin (Spain). Environ. Geol. 54, 963–977.
Lardner, R. 2013. Medslik v. 5.3.7 User Manual, Oceanography Centre, University of Cyprus.
Lardner, R.W., Zodiatis, G., 1998. An operational oil spill model in the Levantine Basin (Eastern Mediterranean Sea). Int. Symp. Mar. Pollut. 10, 5–9.
Lardner, R., Zodiatis, G., Hayes, D., Pinardi, N. 2006. Application of the MEDSLIK oil spill model to the Lebanese spill of July 2006. European Group of Experts on satellite monitoring of sea based oil pollution, European Communities ISSN 1018-5593.
MacFarlane, G.R., Burchett, M.D., 2003. Assessing effects of petroleum oil on intertidal invertebrate communities in Sydney HArbour: preparedness pays off. Aust. J. Ecotoxicol. 9, 29–38.
Mackay, D., Paterson, S., Trudel, K. 1980. A mathematical model of oil spill behavior. Environment Canada Report EE-7.
Mackay, D., Buist, I., Mascarenhas, R., Paterson, S. 1980. Oil spill processes and models. Environment Canada Report EE-8.
Malanotte-Rizzoli, P., Bergamasco, A., 1991. The wind and thermally driven circulation of the eastern Mediterranean Sea. Part II: the Baroclinic case. Dyn. Atmosph. Oceans 15, 355–419.
Marshall, D., 1995. Influence of topography on the large-scale ocean circulation. J. Phys. Oceanogr. 25, 1622–1635.
McCullagh, M.J. 1998. Quality, use and visualisation in terrain modeling. In: Lane, S.N., Richards, K.S., Chandler, J.H. (Eds.), Landform Monitoring, Modeling and Analysis, John Wiley & Sons, Chichester, pp. 95–117.
Murthy, C.S., Raju, P.V., Bradrinath, K.V.S., 2003. Classification of wheat crop with multi-temporal images: performance of maximum likelihood and artificial neural networks. Int. J. Remote Sens. 24, 4871–4890.
Oddo, P., Adani, M., Pinardi, N., Fratianni, C., Tonani, M., Pettenuzzo, D., 2010. A nested Atlantic-Mediterranean Sea general circulation model for operational forecasting. Ocean Sci. 5, 461–473. http://dx.doi.org/10.5194/os-5-461-2009.
Othman, I., Al-Masri, M.S., Al-Rayyes, A.H., 2000. Sedimentation rates and pollution history of the eastern Mediterranean Sea: Syrian coast. Sci. Total Environ. 248, 27–35.
Palinkas, L.A., Downs, M.A., Petterson, J.S., Russell, J., 1993a. Social, cultural, and psychological impacts of the Exxon Valdez oil spill. Hum. Organ. 52, 1–13.
Palinkas, L.A., Petterson, J.S., Russell, J., Downs, M.A., 1993b. Community patterns of psychiatric disorders after the Exxon Valdez oil spill. Psychiatry 150, 1517–1523.
Panagiotakis, C., Kokinou, E. 2014. Automatic enhancement and detection of active sea faults from bathymetry. In: 22nd International Conference on Pattern Recognition, 24–28 August, Stockholm, Sweden, Paper TuBT3, p.19.
Pavlakis, P., Tarchi, D., Siber, A.J., 2001. On the monitoring of illicit vessel discharges using spaceborne sar remote sensing – a reconnaissance study in the Mediterranean sea. Ann. Telecommun. 56, 700–718.
Peterek, A., Schwarze, J., 2004. Architecture and Late Pliocene to recent evolution of outer-arc basins of the Hellenic subduction zone (south-central Crete, Greece). J. Geodyn. 38, 19–56.
Peters, L.D., Shaw, J.P., Nott, M., O'Hara, S.C.M., Livingstone, D.R., 1999. Development of cytochrome P450 as a biomarker of organic pollution in Mytilus sp.: field studies in United Kingdom ('Sea Empress' oil spill) and the Mediterranean Sea. Biomarkers 4, 425–441.
Petterson, C.H., Rice, S.D., Short, J.W., Esler, D., Bodkin, J.L., Ballachey, B.E., Irons, D.R., 2003. Long-term ecosystem response to the Exxon Valdez oil spill. Science 302, 2082–2086.
Piatt, J.F., Anderson, P., 1996. Response of common Murres to the Exxon Valdez oil spill and long-term changes in the Gulf of Alaska marine ecosystem. Am. Fish. Soc. Symp. 18, 720–737.

Pinardi, N., Coppini, G., MFSTEP partners. 2007. Mediterranean ocean forecasting system: towards environmental predictins-(MFSTEP). In: EurOCEAN 2004 Proceedings, 388, ISBN 92-894-7727-X, European Communities.

Pope, R., Wilkinson, K., Skourtsos, E., Triantaphyllou, M., Ferrier, G., 2008. Clarifying stages of alluvial fan evolution along the Sfakian piedmont, southern Crete: new evidence from analysis of post-incisive soils and OSL dating. Geomorphology 94, 206–225.

Postma, G., Drinia, H., 1993. Architecture and sedimentary facies evolution of a marine, expanding outer-arc half-graben (Crete, late Miocene). Basin Res. 5, 103–124.

Pye, K., 1992. Aeolian dust transport and deposition over Crete and adjacent parts of the Mediterranean Sea. Earth Surf. Process. Landf. 17, 271–288.

Roberts, G., Peace, D., 2007. Hydrocarbon plays and prospectivity of the Levantine Basin, offshore Lebanon and Syria from modern seismic data. GeoArabia 12, 99–124.

Rooney, A.H., Ledwin, J. 1989. A priority approach to regional environmental sensitivity mapping. In: Fate and Effects of Oil Spills, Proceedings of the 1989 Oil Spill Oil Conference, USEPA—API.

Sætren, T.G. 2007. Offshore blow-out accidents: an analysis of causes of vulnerability exposing technological systems to accidents. MSc Thesis, Oslo, pp. 125.

Sammarco, P.W., Kolian, S.R., Warby, R.A.F., Bouldin, J.L., Subra, W.A., Porter, S.A., 2013. Distribution and concentrations of petroleum hydrocarbons associated with the BP/Deepwater Horizon Oil Spill, Gulf of Mexico. Mar. Pollut. Bull. 73, 129–143.

Shen, H.T., Yapa, P., Petroski, M., 1987. A simulation model for oil spill transport in lakes. Water Resour. Res. 23, 1949–1957.

Sofianos, Skliris, N., Mantziafou, A., Lascaratos, A., Zodiatis, G., Lardner, R., Hayes, D., Georgiou, G., 2006. Nesting operational forecasting models in the Eastern Mediterranean: active and slave mode. Ocean Sci. Discuss. 3, 1225–1254.

Strozyk, F., Huhn, K., Strasser, M., Krastel, S., Kock, I., Kopf, A., 2009. New evidence for massive gravitational mass-transport deposits in the southern Cretan Sea, eastern Mediterranean. Mar. Geol. 263, 97–107.

Sydney Morning Herald, 1999, Too Crude; News Review (06.08.99).

Theocharis, A., Georgopoulos, D., Lascaratos, A., Nittis, K., 1993. Water masses and circulation in the central region of the Eastern Mediterranean: Eastern Ionian, South Aegean and Northwest Levantine, 1986–1987. Deep-Sea Res. II 40, 1121–1142.

Theocharis, A., Balopoulos, E., Kioroglou, S., Kontoyannis, H., Iona, A., 1999. A synthesis of the circulation and hydrography of the South Aegean Sea and the Straits of the Cretan Arc (March 1994–January 1995). Progress Oceanog. 44, 469–509.

Tonani, M., Pinardi, N., Dobricic, S., Pujol, I., Fratianni, C., 2008. A high-resolution free-surface model of the Mediterranean Sea. Ocean Sci. 4, 1–14. http://dx.doi.org/10.5194/os-4-1-2008.

Torgrimson, G. 1980. The on-scene spill model: a user's guide. Tech. Report, Haz. Mat. Response Branch, National Oceanic and Atmospheric Administration, Seattle, WA.

Triantafyllou, G., Korres, G., Petihakis, G., Pollani, A., Lascaratos, A., 2003. Assessing the phenomenology of the Cretan Sea shelf Area using coupling modelling techniques. Ann. Geophys. 21, 237–250.

Tronczynski, J., Munschy, C., Héas-Moisan, K., Guiot, N., Truquet, I., Olivier, N., Men, S., Furant, A., 2004. Contamination of the Bay of Biscay by polycyclic aromatic hydrocarbons (PAHs) following the T/V "Erika" oil spill. Aquat. Living Resour. 17, 243–259.

Tselepides, A., Polychronaki, T., Marrale, D., Akoumianaki, I., Dell'Anno, A., Pusceddu, A., Danovaro, R., 2000. Organic matter composition of the continental shelf and bathyal sediments of the Cretan Sea (NE Mediterranean). Prog. Oceanogr. 46, 311–344.

United States Congress, 1990, Oil Pollution Act of 1990. USC 2701 note, pp. 66.

van Hinsbergen, D.J.J., Meulenkamp, J.E., 2006. Neogene supradetachment basin development on Crete (Greece) during exhumation of the South Aegean core complex. Basin Res. 18, 103–124.

van Vleet, E.S., Reinhardt, S.B., 1983. Inputs and fates of petroleum hydrocarbons in a subtropical marine estuary. Environ. Int. 9, 19–26.

Whitehead, J.A., 1998. Topographic control of oceanic flows in deep passages and straits. Rev. Geophys. 36, 423–440.

Wirtz, K.W., Liu, X., 2006. Integrating economy, ecology and uncertainty in an oil-spill DSS: the prestige accident in Spain, 2002. Estuar., Coast. Shelf Sci. 70, 525–532.

World Bank: Report No. 39787-LB, 2007, Republic of Lebanon, Economic Assessment of Environmental Degradation due to July 2006 Hostilities.

Zodiatis, G., 1991. The hydrological conditions and the circulation in the Cretan Sea during late summer 1987. Ann. Geophys. 9, 233–238.

Zodiatis, G., 1992. On the seasonal variability of the water masses circulation in the NW Levantine Basin – Cretan Sea and flows through the eastern Cretan Arc straits. Ann. Geophys. 9, 12–14.

Zodiatis, G., 1993a. Circulation of the Cretan Sea water masses (Eastern Mediterranean Sea). Oceanol. Acta 16, 107–114.

Zodiatis, G., 1993b. Water mass circulation between the SE Ionian – W Cretan basins throught he western Cretan Arc stratits. Boll. Oceanol. Teorica ed Appl. 11, 61–75.

Zodiatis, G., Lardner, R., Solovyov, D., Panayidou, X., De Dominicis, M., 2012b. Predictions of oil slicks detected from satellite images using MyOcean forecasting data. Ocean Sci. 8, 1105–1115.

Zodiatis, G. et al. 2012. Operational decision support system for marine safety dedicated to oil slicks predictions. In: World Maritime Technology Conference, Saint-Petersburg, 29 May–1 June.

Zodiatis, G., Galanis, G., Nikolaidis, A., Kalogeri, C., Hayes, D., Georgiou, G.C., Chu, P.C., Kallos, G., 2014a. Wave energy potential in the Eastern Mediterranean Levantine Basin. an integrated 10-year study. Renew. Energy 69, 311–323.

Zodiatis, G., Lardner, R., Nicolaidis, A., Stylianou, S., Panayidou, X., Hayes, D., Galanis, G., Georgiou, G. 2014. MyOcean products in the CYCOFOS decision support system for marine safety. In: Proceedings of the 6th Conference on EuroGOOS: Sustainable Operational Oceanography, EuroGOOS Publication No. 30, pp. 290–299, ISBN 978-91-974828-9-9.